Available online at www.sciencedirect.com
ScienceDirect
Journal of Photochemistry and Photobiology A: Chemistry 185 (2007) 62–66
Journal of Photochemistry and Photobiology A:Chemistry
www.elsevier.com/locate/jphotochem

Biocompatible protoporphyrin IX-containing nanohybrids with potential applications in photodynamic therapy

Giorgos Kantonis, Markos Trikeriotis, Demetrios F. Ghanotakis *

Department of Chemistry, University of Crete, 71409 Heraklion, Crete, Greece

Received 25 January 2006; received in revised form 4 May 2006; accepted 13 May 2006
Available online 21 June 2006

Abstract

Protoporphyrin IX was immobilized in the interlayer region of Mg–Al layered double hydroxides in order to produce biocompatible nanohybrids that could find applications in photodynamic therapy. Protoporphyrin IX and perfluoroheptanoic acid were also cointercalated to produce nanohybrids that combine the oxygen dissolving properties of perfluorocarbons with the photodynamic effect of the porphyrin. The various nanohybrids were characterized by using X-ray diffraction, Fourier transformed infrared spectroscopy, ultraviolet-visible spectroscopy and thermogravimetric analysis. In addition to the intercalation of protoporphyrin IX in the interlayer region of the layered double hydroxides, the X-ray diffraction pattern also showed that intercalation of perfluoroheptanoic acid resulted in the formation of a bilayer between the inorganic layers. Photooxidation experiments using substrates such as imidazole, 2,3-dimethyl-2-butene or linoleic acid, demonstrated the generation of singlet oxygen by these nanohybrids.

Keywords: Layered double hydroxide; Protoporphyrin IX; Photodynamic therapy; Perfluoroheptanoic acid

1. Introduction

Conventional cancer therapies include radiation, chemotherapies, surgery or combinations of them, that usually have important side effects. An alternative is photodynamic therapy (PDT), a treatment modality that is becoming very common against various forms of cancer [1]. In PDT cancer cells are destroyed by reactive oxygen species, mostly singlet oxygen, which is produced with the aid of a photosensitizer and light. Thus, the success of PDT is based on the correct regulation of these three factors: photosensitizer, light and oxygen.

Photosensitization provides a simple and controllable method for the production of singlet oxygen [2]. The photosensitizer molecule is excited by light at high quantum yields and then produces singlet oxygen via energy transfer to molecular oxygen. Porphyrin derivatives, chlorins and phthalocyanines are the most frequently used photosensitizers in PDT [3]. Protoporphyrin IX (ppIX) is a second generation photosensitizer and it is used as an endogenous photosensitizer that is produced in the body by the conversion of topically applied 5-aminolevoulinic acid [4].

The availability of oxygen is also crucial for the efficacy of PDT [5,6]. Under hypoxic conditions cell photoinactivation is totally abolished. As oxygen concentration is a rate limiting factor for the production of singlet oxygen it is important to maintain high oxygen concentrations in solution. A way to achieve this involves the use of perfluorocarbons (PFCs), which are compounds with all aliphatic protons substituted by atoms of fluorine. PFCs can dissolve 20 times more oxygen than water and two to three times more than corresponding hydrocarbons [7]. Their remarkably high gas dissolving capacities along with their chemical and biological inertness make them unique carriers for oxygen delivery in tissues [7–9]. Among perfluorinated fatty acids with different chain lengths, perfluoroheptanoic acid (PFHA) is less toxic and is rapidly eliminated by the body [10,11].

Layered double hydroxides (LDHs) or hydrotalcite-like compounds are synthetic clay materials that form successive layers of metal hydroxides, separated by layers consisting of anions and water [12]. The metal hydroxide layers are positively charged and have similar structure to brucite with a thickness of 4.8 Å. LDHs are represented by the general formula

* Corresponding author. Tel.: +30 2810 393634; fax: +30 2810 393601.
E-mail address: ghanotakis@chemistry.uoc.gr (D.F. Ghanotakis).

1010-6030/$ – see front matter © 2006 Elsevier B.V. All rights reserved.
doi:10.1016/j.jphotochem.2006.05.012

$[M_x^{2+}M_y^{3+}(OH)_{2x+2y}]A_{y/n}^{n-}\cdot zH_2O$, where M^{2+} and M^{3+} are di- and tri-valent metal cations, respectively, and A^{n-} is the interlayer anion. Several organic–inorganic hybrid materials based on LDH have been produced by a simple ion exchange reaction of the interlayer anion [13–15]. These materials are often used as catalysts for chemical conversions [16]. Porphyrins and phthalocyanines have also been intercalated in LDHs [17] and other clays, like smectite, for catalytic purposes [18,19] or for the formation of photocatalytic assemblies [20]. Additionally, hemin was immobilized on smectite to produce a heme-protein model as it could bind oxygen and carbon monoxide [21].

Besides their ion-exchange and catalytic properties, LDHs have been proven to be promising drug delivery vectors [22,23]. LDHs can enter cells and then release the interlayer anions either by ion exchange with cellular anions or by dissolution of the metal hydroxide layers in the acidic environment of the lysosome. Additionally, surface modification could lead to targeted drug delivery to specific cells or organs. Thus, LDHs have been used as carriers in drug delivery and controlled release systems for several anticancer drugs like camptothecin [24], folinic acid and methotrexate [25] and for anti-inflammatory drugs like ibuprofen [26] and naproxen [27].

In this study ppIX was immobilized on layered double hydroxides in order to produce biocompatible nanohybrids that could find application in photodynamic therapy. The immobilized ppIX was able to produce singlet oxygen when it was irradiated with visible light and was catalytically active against various substrates. Nanohybrids containing both ppIX and PFHA were also synthesized. These materials combine the drug delivery properties of LDHs with the photodynamic effect caused by ppIX and the high oxygen solubility of O_2 in perfluorocarbons. As a result, improved PDT can be achieved if these nanohybrids successfully deliver their contents into tumor cells.

2. Experimental

2.1. Materials

Magnesium nitrate hexahydrate 98%, 4-(1,1,3,3-tetramethylbutyl)phenyl–polyethylene glycol (Triton X-100) and 6-O-(*N*-heptylcarbamoyl)-methyl-α-D-glucopyranoside 90% (Hecameg) were purchased from Sigma. Protoporphyrin IX disodium salt, perfluoroheptanoic acid 99% and 2,3-dimethyl-2-butene 98% were purchased from Aldrich. Sodium hydroxide pellets 99%, aluminum nitrate nonahydrate 98.5% and $CDCl_3$ 99.8% for NMR were purchased from Merck. Dichloromethane 99.9% and linoleic acid 90% were purchased from Fluka. Imidazole 99% was purchased from Riedel-de Haen. All chemicals were used without further purification.

2.2. Synthesis of LDH and LDH nanohybrids

Mg–Al–NO_3 layered double hydroxides with Mg/Al ratio 2/1 and 3/1 were prepared by coprecipitation at constant pH and at room temperature according to Miyata [28]. A solution containing $Mg(NO_3)_2\cdot6H_2O$ (30.8 g, 120 mmol) and $Al(NO_3)_3\cdot9H_2O$ (22.5 g, 60 mmol) in deionized water (200 cm^3) and a solution containing NaOH (16.0 g, 400 mmol) in deionized water (200 cm^3) were added dropwise to deionized H_2O (200 cm^3) so as the pH was maintained at 10 ± 0.5 at room temperature. After the addition was completed, the resulting slurry was aged for 1 day at room temperature. The suspension was then centrifuged at $12{,}000 \times g$ for 15 min and washed several times with deionized water. LDH was stored as a suspension in order to prevent crystal aggregation. All solutions during synthesis were decarbonated under N_2 flow for 20 min.

LDH nanohybrids were synthesized via anion exchange. For the preparation of the nanohybrid of LDH with ppIX (LDH–ppIX), ppIX (91 mg, 0.15 mmol) and $[Mg_3Al(OH)_8]$-NO_3 (50 mg) were added in decarbonated water (50 cm^3). The pH was adjusted to 9.0 and the mixture was stirred at room temperature for 2 days. The resulting nanohybrid was collected by centrifugation at $12{,}000 \times g$ for 15 min and after two washing steps with deionized water it was filtered under vacuum and dried in air.

PpIX and PFHA were co-immobilized on LDH with Mg/Al ratio 2/1 at the same conditions as above. The reaction mixture contained ppIX (91 mg, 0.15 mmol) and PFHA (164 mg, 0.45 mmol) in decarbonated water (50 cm^3) and the resulting nanohybrid (LDH–ppIX–PFC) was collected by centrifugation after 4 days.

The nanohybrid of LDH with PFHA (LDH–PFC) was prepared by dissolving PFHA (0.36 g, 1 mmol) in an aqueous solution (50 cm^3) containing Hecameg (0.25 g, 7.5 mmol). After the addition of $[Mg_3Al(OH)_8]NO_3$ (0.20 g) the pH was adjusted to 10.0 and the solution was stirred for 2 days.

2.3. Characterization

Powder X-ray diffraction (XRD) patterns were recorded on a Rigaku RINT 2000 powder diffractometer, using Cu Kα radiation ($\lambda = 1.54$ Å) at 40 kV and 178 mA. Fourier transformation infrared (FT-IR) spectra were recorded using KBr disks on a Perkin-Elmer 1760X FT-IR spectrometer. Ultraviolet-visible (UV–vis) spectra were recorded using a SLM-Aminco DW2000 spectrometer. The ^1H NMR spectra were recorded on a 300 MHz MSL Bruker spectrometer. Thermogravimetric analysis was carried out using a Perkin-Elmer Pyris Diamond TG/DTA, at 10 °C/min. Immobilized ppIX was quantified by dissolving a known amount of each nanohybrid in ethanol/1 M HCl 4/1 and then recording the absorbance at 558 nm.

2.4. Photocatalytic activity measurement

The activity of the immobilized ppIX was assayed by monitoring the O_2 uptake during the photooxidation of imidazole, 2,3-dimethyl-2-butene or linoleic acid. Oxygen concentration was monitored by a Yellow Spring Instruments (model 5300) Clark-type electrode. A small amount of ppIX, LDH–ppIX or LDH–ppIX–PFC was dissolved in deionized water (15 cm^3) containing Triton X-100 (0.15 cm^3) and the solution was equilibrated with pure O_2 for 15 min. The exact concentration of ppIX

present in each solution was determined as described above. For each photooxidation reaction 3.0 cm^3 of oxygenated ppIX solution were placed on the Clark electrode cell and 0.3 μmol of imidazole or 2,3-dimethyl-2-butene, or 0.03 μmol of linoleic acid were added. The reaction was initiated when two slide projector lamps were turned on.

The product of 2,3-dimethyl-2-butene photooxidation was characterized with ^{1}H NMR spectroscopy. Each nanohybrid, or free ppIX, and the substrate were dissolved in $CHCl_3$. The reaction mixture was then irradiated under O_2 atmosphere, at 0 °C for 10 min. Before recording the ^{1}H NMR spectrum, the solvent was evaporated and the sample was dissolved in $CDCl_3$.

3. Results and discussion

3.1. Characterization

Successful intercalation of ppIX and PFHA was confirmed by powder X-ray diffraction (Fig. 1). As calculated from the mean value of the first, second and third order peaks, the *d*-spacing is 23.0 Å for LDH–PFC, 23.6 Å for LDH–ppIX and 23.9 Å for LDH–ppIX–PFC (Table 1). In the case of LDH–PFC the interlayer distance (≈18.0 Å) is large enough to accommodate a bilayer of PFHA molecules. The sharp and intense peaks of the XRD pattern suggest a well-ordered structure giving additional support to this assumption. Protoporphyrin containing nanohybrids seem to be less ordered probably due to a different orientation of the porphyrin rings in the interlayer space. The *d*-spacing for LDH–ppIX is in good agreement with previously reported clay-porphyrin hybrids [18,19].

The infrared spectra (Fig. 2) give further evidence of the intercalation of ppIX, especially concerning the state of the carboxylic group [29]. The asymmetric stretch of the carboxylate groups of perfluoroheptanoic anion and ppIX appear at 1670 and 1550 cm^{-1}, respectively. Both peaks appear in the spectrum of LDH–ppIX–PFC. The symmetric stretch of the carboxylate groups is located near 1420 cm^{-1} in all three spectra. Furthermore, several peaks characteristic of ppIX appear in the region between 1250 and 850 cm^{-1}. A number of peaks characteristic of the C–F bond [30] appear in the spectra of LDH–PFC and LDH–ppIX–PFC in the region between 1000 and 1300 cm^{-1}. These results show that both ppIX and PFHA are in the ionized form in the interlayer space of the nanohybrid and that they are immobilized by electrostatic interactions with the metal hydroxide layers. The IR spectrum of LDH–ppIX–PFC proves that ppIX and PFHA are cointercalated in the LDH nanohybrid.

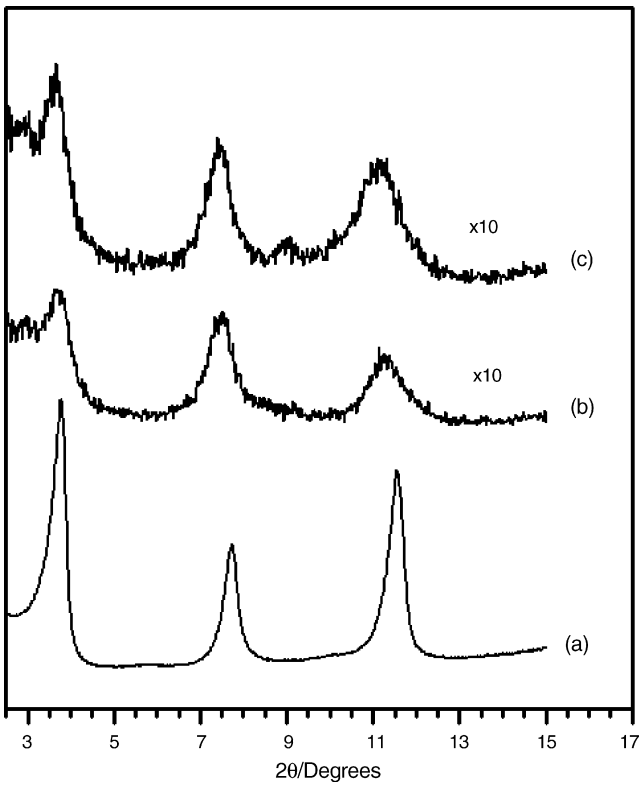

Fig. 1. X-ray diffraction patterns of the three nanohybrids: (a) LDH–PFC, (b) LDH–ppIX, (c) LDH–ppIX–PFC.

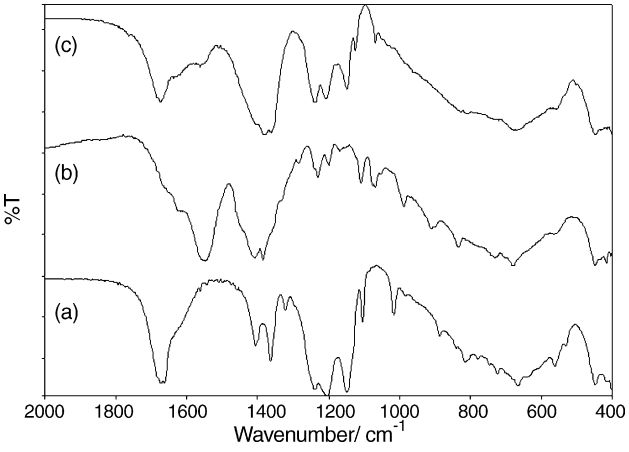

Fig. 2. Infrared spectra of the three nanohybrids: (a) LDH–PFC, (b) LDH–ppIX, (c) LDH–ppIX–PFC.

Table 1
XRD and compositional data of the nitrate clay and the three nanohybrids

Nanohybrids	*d* values (Å)			Water (%)	PFHA (%)	pp IX (%)	
	d_{003}	d_{006}	d_{009}			UV	TGA
LDH–NO_3	8.7	4.4	3.0	10	–	–	–
LDH–PFC	23.3	11.4	7.6	4	54	–	–
LDH–ppIX	23.9	11.8	7.8	11	–	18	23
LDH–ppIX–PFC	24.1	11.8	7.9	4	15	10	11

Although the presence of ppIX or PFHA was evident from the XRD patterns and FTIR spectra, thermal analysis was also necessary to establish the composition of the nanohybrids (Table 1). First, the water content of the nanohybrids was calculated by the weight loss at the first step around 400 K. As expected the hydrophobic PFHA-containing nanohybrids have much less adsorbed water than LDH–NO_3 or LDH–ppIX. In the region between 450 and 700 K the decomposition of the intercalated compounds is observed. LDH–PFC loses 54% (w/w) between 480 and 530 K, which is due to exothermic decomposition of PFHA (not shown). An exothermic process is also observed for the LDH–ppIX–PFC nanohybrid around 500 K (Fig. 3B) and thus the 15% (w/w) loss at this stage corresponds to the amount of PFHA. Both porphyrin containing nanohybrids show endothermic peaks around 630 K that correspond to the decomposition of protoporphyrin IX (Fig. 3). The weight loss at this stage is 23% (w/w) for LDH–ppIX and 11% (w/w) for LDH–ppIX–PFC.

The nanohybrids were further characterized by using UV–vis spectroscopy. As shown in Fig. 4, both nanohybrids have typical porphyrin spectra with the Soret band at 410 nm and additional Q bands at 505, 540 and 580 nm. Some broadening observed mostly in the region of the Soret band can be attributed to partial aggregation of ppIX molecules. The absorbance of ppIX was also used to quantify the immobilized ppIX on each nanohybrid. The extinction coefficient of ppIX at 558 nm, in a mixture of ethanol/1 M HCl 4/1 was calculated by measuring a series of known samples and was found to be $(1.62 \pm 0.01) \times 10^4\ cm^{-1}\ M^{-1}$. As shown in Table 1 the nanohybrid LDH–ppIX contained 18% (w/w) ppIX, while LDH–ppIX–PFC contained 10% (w/w) ppIX. These values are in good agreement with the thermal analysis results.

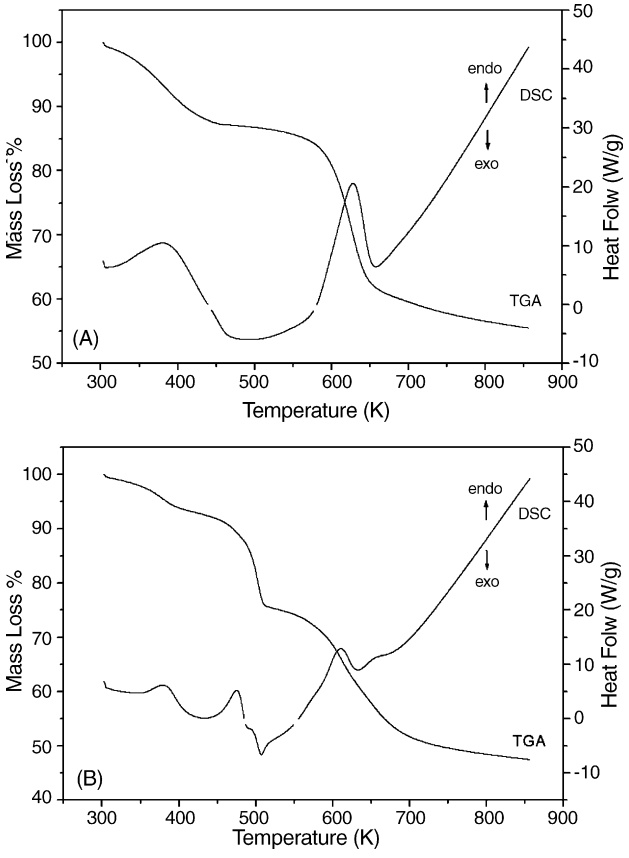

Fig. 3. TGA and DSC diagrams of the porphyrin containing nanohybrids: (A) LDH–ppIX, (B) LDH–ppIX–PFC.

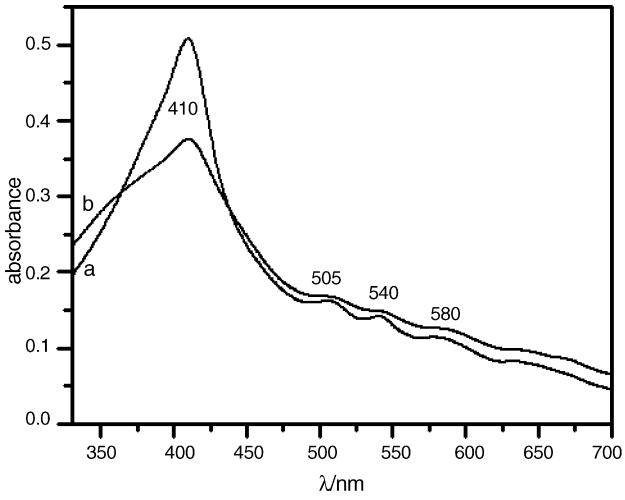

Fig. 4. Ultraviolet-visible spectra of the nanohybrids in water: (a) LDH–ppIX, (b) LDH–ppIX–PFC.

3.2. Photocatalytic activity

The ability of the nanohybrids to produce singlet oxygen and oxidize various substrates was compared with that of free ppIX. The results are presented in Table 2. Free ppIX and both the nanohybrids can oxidize imidazole, 2,3-dimethyl-2-butene and linoleic acid. Control experiments showed that in the absence of ppIX or substrate there was no significant O_2 consumption. The three substrates that were used are different in many ways. Imidazole is water soluble, while the other two are not. In the presence of the non-ionic surfactant Triton X-100 2,3-dimethyl-2-butene becomes easily soluble while linoleic acid is only slightly soluble. These differences are reflected in the reaction rates during photooxidation. When imidazole is used as substrate the reaction is five to nine times faster with free ppIX compared to LDH–ppIX and LDH–ppIX–PFC, respectively. In the presence of hydrophobic substrates the nanohybrid LDH–ppIX–PFC gives the faster reactions. Especially in the case of linoleic acid the reaction with LDH–ppIX–PFC as catalyst is four to seven times faster than with LDH–ppIX and free ppIX, respectively.

Table 2
Reaction rate for the oxidation of different substrates (moles $O_2 \times min^{-1} \times [ppIX]^{-1} \times 10^{-3}$)

Catalyst	Substrate		
	Imidazole	2,3-Dimethyl-2-butene	Linoleic acid
Protoporphyrin IX	20.4	6.43	0.13
LDH–ppIX	4.12	3.79	0.19
LDH–ppIX–PFC	2.48	8.30	0.87

These results suggest that the polarity of the catalyst and the substrate determine the reaction rate. Thus, the oxidation of linoleic acid with a hydrophobic catalyst, like the perfluorocarbon modified nanohybrid, is much faster compared to the oxidation with free ppIX. On the other hand hydrophilic imidazole reacts much faster with water soluble, free ppIX than with the nanohybrids. The fact that the reaction takes place in a micellar solution may also be responsible for the substrate selectivity. When the catalyst and the substrate are distributed both in the hydrophobic microenvironment of the micelle core or both in the bulk solution, it is more possible that singlet oxygen will react with a substrate molecule before it is quenched in other ways. This is not likely to happen if the catalyst and the substrate are distributed separately.

When 2,3-dimethyl-2-butene was used as a substrate, the photooxidation product was identified by using ^{1}H NMR spectroscopy (data not shown). Both nanohybrids and the free ppIX gave 2,3-dimethyl-3-hydroperoxy-1-butene as the final photooxidation product.

4. Conclusion

Protoporphyrin IX containing nanohybrids were synthesized by a simple ion-exchange reaction of the starting material LDH–NO_3. These nanohybrids produce singlet oxygen when they are excited by visible light resulting in the oxidation of various substrates. Hydrophobization of the nanohybrids makes them more active against hydrophobic substrates and probably enhances their localization in non-polar environments like micelles or possibly biological membranes. A more complex nanohybrid was synthesized, containing both ppIX and PFHA, to take advantage of the remarkably high solubility of O_2 in perfluorocarbons and overcome the problem of O_2 depletion during the photooxidation. These properties of the synthesized nanohybrids, along with the drug delivery ability of LDHs, make them very promising photodynamic therapy agents. In vitro studies are now in progress in order to investigate the ability of these nanohybrids to load target cells with a photosensitizer (ppIX) and O_2, and thus facilitate the destruction of these cells by singlet O_2 generated by illumination.

Acknowledgments

The authors would like to thank Prof. S. Anastasiadis (University of Thessaloniki) for the XRD and Prof. E. Giannelis (Cornell University) for helpful discussions. This work was supported by the Greek Ministry of National Education and Religious Affairs (Program Herakleitos).

References

[1] B.W. Henderson, T.J. Dougherty, Photochem. Photobiol. 55 (1992) 145–157.
[2] I.E. Kochevar, R.W. Redmond, Methods Enzymol. 319 (2001) 20–28.
[3] M.R. Detty, S.L. Gibson, S.J. Wagner, J. Med. Chem. 47 (2004) 3897–3915.
[4] J.C. Kennedy, R.H. Pottier, D.C. Pross, J. Photochem. Photobiol. B: Biol. 6 (1990) 143–148.
[5] J. Fuchs, J. Thiele, Free Radic. Biol. Med. 24 (1998) 835–847.
[6] W.M. Sharman, C.M. Allen, J.E. van Lier, Methods Enzymol. 319 (2001) 376–400.
[7] J.G. Riess, Chem. Rev. 101 (2001) 2797–2919.
[8] R.M. Winslow, Adv. Drug Deliv. Rev. 40 (2000) 131–142.
[9] O.P. Habler, K.F. Messmer, Adv. Drug Deliv. Rev. 40 (2000) 171–184.
[10] N. Kudo, E. Suzuki, M. Katakura, K. Ohmori, R. Noshiro, Y. Kawashima, Chem. Biol. Interact. 134 (2001) 203–216.
[11] K. Ohmori, N. Kudo, K. Katayama, Y. Kawashima, Toxicology 184 (2003) 135–140.
[12] F. Cavani, F. Trifiro, A. Vaccari, Catal. Today 11 (1991) 173–301.
[13] S. Carlino, Solid State Ionics 98 (1997) 73–84.
[14] M. Meyn, K. Beneke, G. Lagaly, Inorg. Chem. 29 (1990) 5201–5207.
[15] S.Y. Kwak, Y.J. Jeong, J.H. Choy, Solid State Ionics 151 (2002) 229–234.
[16] T.J. Pinnavaia, M. Chibwe, V.R.L. Constantino, S.K. Yun, Appl. Clay Sci. 10 (1995) 117–129.
[17] I.-Y. Park, K. Kuroda, C. Kato, Chem. Lett. (1989) 2057–2058.
[18] M. Chibwe, L. Ukrainczyk, S.A. Boyd, T.J. Pinnavaia, J. Mol. Catal. A: Chem. 113 (1996) 249–256.
[19] Z. Tong, T. Shichi, K. Takagi, Mater. Lett. 57 (2003) 2258–2261.
[20] D.S. Robins, P.K. Dutta, Langmuir 12 (1996) 402–408.
[21] T. Itoh, T. Yamada, Y. Kodera, A. Matsushima, M. Hiroto, K. Sakurai, H. Nishimura, Y. Inada, Bioconjugate Chem. 12 (2001) 3–6.
[22] J.H. Choy, S.Y. Kwak, Y.J. Jeong, J.S. Park, Angew. Chem. Int. Ed. Engl. 39 (2000) 4042–4045.
[23] K.M. Tyner, M.S. Roberson, K.A. Berghorn, L. Li, R.F. Gilmour Jr., C.A. Batt, E.P. Giannelis, J. Control. Rel. 100 (2004) 399–409.
[24] K.M. Tyner, S.R. Schiffman, E.P. Giannelis, J. Control. Rel. 95 (2004) 501–514.
[25] J.H. Choy, J.S. Jung, J.M. Oh, M. Park, J. Jeong, Y.K. Kang, O.J. Han, Biomaterials 25 (2004) 3059–3064.
[26] V. Ambrogi, G. Fardella, G. Grandolini, L. Perioli, Int. J. Pharm. 220 (2001) 23–32.
[27] A.I. Khan, L. Lei, A.J. Norquist, D. O'Hare, Chem. Commun. (2001) 2342–2343.
[28] S. Miyata, Clays Clay Miner. 23 (1975) 369–375.
[29] M. Borja, P. Dutta, J. Phys. Chem. 96 (1992) 5434–5444.
[30] J.A. Dean, Lange's Handbook of Chemistry, McGraw-Hill, New York, 1999.